

# DOPPLER BASED DETECTION OF MULTIPLE TARGETS IN PASSIVE WIFI RADAR USING UNDERDETERMINED BLIND SOURCE SEPARATION

Qingchao Chen<sup>1</sup>, Bo Tan<sup>2</sup>, Karl Woodbridge<sup>1</sup> and Kevin Chetty<sup>1</sup>

<sup>1</sup> University College London, London, UK

<sup>2</sup> University of Coventry, UK

{qingchao.chen.13, k.woodbridge, k.chetty}@ucl.ac.uk, bo.tan@coventry.ac.uk

## ABSTRACT

Passive approaches for detecting and localizing people in wireless environments have attracted significant attention because of its diverse application in healthcare, security and robotics in recent years. However, within indoor environments multiple people moving in close proximity to each other often impedes the utility of such approaches. In this paper we present a new method for identifying multiple human targets in Wi-Fi passive radar systems using only a single receive channel to detect Doppler returns. The technique is based on tree-structure sparse underdetermined blind source separation and utilizes proximal alternating methods in a convex optimization field. Firstly, we show proof-of-principle simulation results for two targets moving within a typical indoor scenario and compare the results with those from the well-known independent component analysis (ICA). Secondly, we validate the simulation outputs using real-world experimental data. The results demonstrate the effectiveness of the proposed technique for device-free detection of multiple targets in the indoor wireless landscape.

**Index Terms**— Passive Wi-Fi radar, Multiple target detection, Underdetermined Blind Source Separation, proximal alternating Linearized minimization

## 1. INTRODUCTION

Passive radar systems make use of *signals of opportunity* of such as GSM[1], Wi-Fi [2] [3, 4] and DAB/DVB-T [5] to detect and track targets of interest. They essentially consist of a series of synchronized radio receivers which compare the echoes from moving targets to the original unaltered transmission signal. The receive-only nature of passive radar systems means that they are low-cost, covert, and operate license-free. Recently development in [6] shows that passive radar system can achieve high frequency (Doppler) resolution. Based on the high-resolution characteristic, indoor device-free localization using Doppler-only passive Wi-Fi radar has been demonstrated to localize and track single targets[3]. Also passive Wi-Fi radar has been utilized to track multiple targets utilizing the Inverse Synthetic Aperture Radar (ISAR) techniques [23]. In addition, human motion gesture detection and recognition have<sup>i</sup> also been

shown [7, 8]. However, the multiple targets detection by passively using indoor wireless signals like WiFi is still rare due to the lack of range resolution.

For multiple-target detection methods, some active radar techniques utilize bespoke waveforms with large bandwidths to provide high range resolutions[9, 10]. Other techniques utilize Constant False Alarm Rate (CFAR) methods to search the range-Doppler surface[11]. The resolution of passive Wi-Fi radar itself is limited by its 16MHz bandwidth which gives a relatively coarse range resolution of approximately 12 meters. This makes the detection of multiple targets based only on ranging data very difficult.

Another approach to tackle the multiple target problem is blind source separation (BSS). In the field of BSS, where multiple receivers are used to recover a mixture of different sources, independent component analysis (ICA) methods are used extensively for a range of applications including EEG [12], and image separation[13]. With advancements in sparse representation, the iterative shrinkage-threshold algorithm has proven to be popular in separating mixed music with different regularization terms[14]. Recently, the sparsity based Generalized Morphological Component Analysis (GMCA) method has been the subject of much interest in hyperspectral data analysis [15], as the better representation under hybrid basis. Underdetermined BSS (UBSS) [16] is a more practical extension of the BSS problem, as it utilizes fewer receivers to reconstruct the original sources. To our knowledge, sparsity based UBSS method has not been applied to Doppler signal separation in radar. In this paper, we proposed Tree-structured sparse-Undetermined Blind Source Separation (TUBSS) method is investigated for multiple-target detection in Doppler only passive Wi-Fi radar. TUBSS can better separate mixed Doppler echoes induced by multiple targets than the one which directly performs Doppler estimation. In addition, compared with UBSS method, TUBSS is able to better separate multiple targets' Doppler echoes using fewer receivers under interference. The results shown in this paper is based on the use of only one surveillance receiver. However the technique can be extended to multiple surveillance receivers.

The rest of the paper is organized as following: Section II describes the signal model and Doppler detection of passive WiFi Radar. UBSS and proposed TUBSS methods are introduced in Section III; Section IV outlines and analysis simulation and experimental results; Conclusion is given in Section V.

## 2. SIGNAL MODEL AND DOPPLER DETECTION IN PASSIVE WIFI RADAR

Passive Wi-Fi radar utilizes the existing Wi-Fi access points (APs) as transmitters of opportunity. The reference signal  $ref(t)$ , is regarded as the linear combination of the ‘clean’ transmitted Wi-Fi signal  $x_{source}(t)$  and the reflections from static objects, characterized by  $p^{th}$  delay,  $\tau_p$  and relevant magnitude  $A_p$ :

$$ref(t) = \sum_p A_p x_{source}(t - \tau_p). \quad (1)$$

Similarly, the signal in the surveillance channel  $sur(t)$ , is composed of echoes from all moving targets in the illuminated area of interest, which can be characterized as the  $p^{th}$  delay  $\tau_p$ , its Doppler shift  $f_{d,p}$  and relevant magnitude  $A_p$ :

$$sur(t) = \sum_p A_p x_{source}(t - \tau_p) e^{j2\pi f_{d,p} t}. \quad (2)$$

In general, a target can be identified by cross correlating the reference and surveillance signals and using a Fast Fourier Transform (FFT) to find the exact delay  $\tau$  and frequency shift  $f$  of the strongest signal. This can be represented by the Cross Ambiguity Function (CAF) as follows[2]:

$$CAF(\tau, f) = \int_{-\infty}^{+\infty} e^{-j2\pi f t} ref^*(t - \tau) sur(t) dt. \quad (3)$$

As the limited bandwidth of the Wi-Fi signal, the range resolution of the Wi-Fi radar is around 12 meters. We can therefore assume the target is in one range bin for each CAF operation. The  $M$  samples of correlation result  $x[m], m \in [0, M - 1]$  in the time domain within a specific range bin  $l_{max}$  is then given by:

$$x[m] = \sum_{n=0}^{N_m-1} ref^*[i_m + n - l_{max}] sur[i_m + n], \quad (4)$$

where  $M$  is the number of batches[17] we divide the signal into,  $N_m$  is the number of data samples in  $m^{th}$  batch and  $i_m$  is the starting sample index of each batch. In contrast to CAF processing, the extracted signal  $x[m]$  is regarded as the input signal for the TUBSS method described in section 3.

## 3. UNDERDETERMINED SPARSE-BLIND SOURCE SEPARATION FOR MULTI-TARGET DETECTION

This section first describes the UBSS model for multi-target detection in passive Wi-Fi radar. The Proximal Alternating Linearized Minimization (PALM) [18] framework is then introduced to estimate unknowns. Finally a TUBSS framework is proposed to deal with the problems of real-time data.

### 3.1 Undetermined BSS Model for Target Separation

In the UBSS model, targets echoes as independent sources since the target’s movements are random and independent, thus it needs  $K$  receivers to separate  $N$  source targets with  $K < N$ . This makes the separation task impractical in the real-life scenario since we cannot usually have the same number of receivers as the number of targets. For the UBSS model in passive radar, after cross-correlation via Eq.(4), the  $M$  samples of  $K$  mixed Doppler signal  $X_k \in \mathcal{C}^{1 \times M}$ , can be described as the linear mixture  $A_{kn} \in \mathcal{C}^{1 \times N}$ , and  $N$  separated Doppler source  $S_n \in \mathcal{C}^{1 \times M}$ , plus additive white Gaussian noise,  $\omega_k$ :

$$X_k = \sum_{n=1}^N A_{kn} S_n + \omega_k. \quad (5)$$

The separation task is to extract the mixing matrix  $A \in \mathcal{C}^{K \times N}$  and the separated sources  $S \in \mathcal{C}^{N \times M}$  given the observed signal mixture  $X \in \mathcal{C}^{K \times M}$ . Intuitively, the support,  $\alpha \in \mathcal{C}^{N \times M}$  of the separated source  $S$  under an Inverse Discrete Fourier Transform (IDFT) basis  $D \in \mathcal{C}^{M \times M}$  should be sparser than each of the mixed signals  $X$ . Accordingly, the UBSS problem becomes a convex optimization problem represented in the matrix form:

$$\begin{aligned} \min_{(A,S)} \frac{1}{2} * \|X - AS\|_2^2 + \lambda \|\alpha\|_1 \\ \text{s.t. } S = \alpha D^T, \end{aligned} \quad (6)$$

where  $T$  is the transpose operator. As the separated signal after correlation is only the Doppler signal, we simply add the  $l_1$ -norm as a constraint to the optimization formula.

### 3.2 Proximal Alternating Algorithm

In equation (6), as the term  $\|\alpha\|_1$  is the non-linear part, the Lipchitz continuity with respect to  $\alpha$  cannot be held. This limits the usage of proximal projection methods. However, the Proximal Alternating Linearized Minimization (PALM) method is introduced in recent research [18, 19], because only the first term  $\frac{1}{2} * \|X - AS\|_2^2$  contains all the variables and its gradient is Lipchitz continuous. Then  $\|\alpha\|_1$ , the non-smooth term, can be solved by soft-threshold methods when the other variables are fixed. The procedures of optimizing  $A$  and  $\alpha$  at the  $t+1$  iteration is summarized as the following.

#### 3.2.1 Compute $\alpha^{t+1}$ using $\alpha^t$ and $A^t$

Initially, the first order partial derivative of the first term  $h = \frac{1}{2} * \|X - AS\|_2^2$  and its Lipchitz constant with respect to  $\alpha$  can be found from:

$$\nabla_{\alpha^t} h = -A^H (X - A\alpha^t D^T) * (D^T)^H, \quad (7)$$

and the Lipchitz constant by:

$$L_{\alpha^t} = \|A^H A D^T (D^T)^H\|_F, \quad (8)$$

where  $H$  is the Hermitian transpose and  $\|\cdot\|_F$  is the Frobenius norm. Then according to [4, 5], through the proximal mapping step and  $l_1$ -norm regularization,  $\alpha^{t+1}$  can be updated by the following equation:

$$\hat{\alpha}^{t+1} = \alpha^t - \frac{1}{L_{\alpha^t}} * \nabla_{\alpha^t} h, \quad (9)$$

and the soft-threshold operator to each element in  $\hat{\alpha}^{t+1}$ :

$$\alpha_f^{t+1} = \text{sign}(\hat{\alpha}_f^{t+1}) * (|\hat{\alpha}_f^{t+1}|, \lambda)^+. \quad (10)$$

### 3.2.2 Compute $A^{t+1}$ using $A^t$ and $\alpha^{t+1}$

The procedure for calculating  $A^{t+1}$  is similar to the previous steps. The first order partial derivative of  $h$  and the Lipchitz constant with respect to  $A$  is computed as:

$$\nabla_{A^t} h = -(X - A^t \alpha^{t+1} D^T) * (D^T)^H * (\alpha^{t+1})^H, \quad (11)$$

with the Lipchitz constant given by:

$$L_{A^t} = \|(\alpha^{t+1}) D^T (D^T)^H (\alpha^{t+1})^H\|_F. \quad (12)$$

Without the non-linear part, the update of  $A^{t+1}$  can be directly obtained by the following:

$$A^{t+1} = A^t - \frac{1}{L_{A^t}} * \nabla_{A^t} h. \quad (13)$$

### 3.3 Tree Structure Based sparse-UBSS (TUBSS) in High-power Interference Scenarios

In real-world scenarios, due to the different ranges of targets, the powers of Doppler echoes vary significantly and the required target Doppler may be masked by other targets or interference. However, we here propose a tree-structure Sparse-UBSS to extract the Doppler sources by estimating a sequence of mixing matrices in multiple steps. The details of the algorithms are summarized in algorithm 1 and 2.

Take the  $N$  targets, TUBSS with one receiver as an example. The input root node is the mixed signal from one receiver and each leaf node with the sparsest frequency spectrum should be chosen as the potential Doppler sources, ready for another separation to the next layer. The stopping criterion for adding more separation siblings is that  $N$  sources are collected and for each source difference between the first two largest frequency coefficient is larger than 3db [20].

---

#### Algorithm 1: Sparse-UBSS Doppler Separation

**Input:** Mixing matrix  $A^0 \in K * N$ , Separated Source Signal  $S^0 \in N * M$ , Iteration Index  $t = 0$ , Mixed signal  $X \in K * M$ , Inverse Discrete Fourier Transform matrix  $D \in M * M$ ;

Calculate  $\alpha^0 = FFT(S^0)$ .

**while until converge do**

$t=t+1$ ;

    Update  $\alpha^{t+1}$  via Eq.(7),(8),(9),(10) with fixed  $A^t$ ;

    Update  $A^{t+1}$  via Eq.(11),(12),(13) with fixed  $\alpha^{t+1}$ ;

**Output:** Estimated  $A$  and  $S = IFFT(\alpha^{t+1})$

---

## 4. RESULTS AND ANALYSIS

In this section, both simulation and real-life experimental data based separation results of passive Wi-Fi radar are presented. In addition, results based the robust ICA and the TUBSS method are compared for the simulation data. Finally, the experimental results using the TUBSS method are shown.

### 4.1 Experiment Set Up and Implementation

For the simulation, the Wi-Fi signals from both the reference and surveillance channel are simulated using a Dell M4700 laptop with Matlab2012b. The Wi-Fi signal is based on the 64-quadrature amplitude modulation (QAM) modulation and encoded by Orthogonal Frequency-Division Multiplexing (OFDM). The length of the simulation signal is 0.5 second with 20 MHz bandwidth at the center frequency of 2.462 GHz. The experimental set up is shown

---

#### Algorithm 2: : Single Channel Tree-structure Sparse-UBSS Doppler Separation

**Input:** Mixing matrix  $A^1 \in 1 * N$ , Separated Source Signal  $S^1 \in N * M$ , Node Index  $i = 0$ , Mixed signal  $X \in 1 * M$ , Potential depth of tree structure  $P$ , Inverse Discrete Fourier Transform matrix  $D \in M * M$ .

**while until converge do**

$i=i+1$ ;

**if**  $i > P$  **then**

**break**;

**if**  $i = I$  **then**

$X^i = X$ ;

        Obtain  $S^i$  via Algorithm 1;

        Add  $S^i$  to  $X^{temp}$ ;

**else**

        Set  $X^i = X^{temp}$ ,  $X^{temp} = NULL$ ;

        Set  $N_i$  the number of mixture of  $X^i$ ;

**if**  $N_i = 0$  **then**

**break**;

        Randomly set  $S_j^i \in N * M$ ,  $A_j^i \in 1 * N$ ;

**for**  $j=1:N_i$  **do**

            Update  $S_{N*(j-1)+1:N*j}^i$  via Algorithm 1 using  $X_j^i$ ;

**for**  $j=1:N_i$  **do**

**for**  $l = N * (j - 1) + 1 : N * j$  **do**

                calculate  $\alpha_l^i = FFT(S_j^i)$ ;

$l_{min} = \min_l \|\alpha_l^i\|_1$ ;

                select the first two largest elements of  $\alpha_{l_{min}}^i$  as  $\beta_{max1}$ ,  $\beta_{max2}$ ;

**if**  $(\beta_{max1} - \beta_{max2}) > 3dB$  **then**

                    Add  $S_j^i$  to target set T;

**else**

                    Add  $S_j^i$  to one of the mixture of  $X^{temp}$ ;

**Output:** Target Set T

---

schematically in figure 3. A Wi-Fi AP is used as the transmitter and the UCL Software Defined Radio based Passive Wi-Fi radar [4] collected the reference and surveillance data using two Yagi antennas with 14 dbi gain.

### 4.2 Simulation Results and Analysis

For the TUBSS, we only use one receiver and one node tree to separate the two sources. For comparison, the robust ICA method [21] is usually carried out using two receivers with the distance between antennas half a wavelength. The following two scenarios were simulated:

**Scenario 1:** Two people are walking at 1m/s away from the receiver and 0.5m/s towards the receiver respectively, with Doppler echo signals with SNR of 2, 5, 8 and 10 db.

**Scenario 2:** Two people are both walking towards the receiver at 1m/s and 0.5m/s respectively with Doppler echo signals with SNR of 2, 5, 8 and 10 db.

TUBSS and the robust-ICA are compared using the Signal Distortion Ratio (SDR) and Signal Interference Ratio (SIR) from BSS evaluation methods [22], as shown in figure 1 and

2. In general, with the increasing power of Doppler echoes, the SDR and SIR of both scenarios are increasing. When the two velocities are in the opposite direction, as the less correlated Doppler signals, the SDR and SIR are higher than the case when the targets are moving in same direction for both methods. In the case of same direction targets, although with only one receiver, the TUBSS slightly outperforms the robust ICA, as the ICA is not so robust for noisy environments and mixtures of target signals with more correlations [16]. It is noted that the ICA performs basically the same as TUBSS at 10db due to less noise for mixtures. The robust ICA performs better than the TUBSS and delivers more accurate estimation of the mixing matrix, due to more receivers and less correlated Doppler signals. The potential reason for the ICA's outperformance when separating velocity of opposite direction may be: it is an easier task to separate Doppler signals with opposite velocity and not to say ICA can use two channels information.

### 4.3 Experiment Results and Analysis

The experimental scenarios is shown in figure 3 and experimental results are shown in figures 4 and 5 respectively. It is noted that we have not included the raw range-Doppler map as in the indoor scenario the target always stays in the first range bin. In this way, we think that the Doppler information from the first range bin can verify and compare with the separation results. Two more scenarios are introduced in experiment:

**Scenario 3:** two targets are walking in opposite directions, close together;

**Scenario 4:** the two targets are walking in opposite directions farther apart.

From the CAF results in figure 4(b) and 5(b), the two scenarios are difficult to separate, due to the ambiguities from interference and the mixed phases of source signals in figure 4(a) and 5(a). Furthermore, due to the longer range from the receiver in scenario 4 the target SNR is very low.

A significant improvement is shown using the TUBSS method. With a one-depth tree structure for **Scenario 3**, the two targets with 0.5 m/s and -0.5m/s can be identified easily from figures 4 (d) and (f). For **Scenario 4**, although one of the echoes has low power, we used a depth-three TUBSS to pick up the Doppler returns, as shown in figures 5(d) and (f). The high-power interference signals with similar frequency are rejected since only the signal whose phase variation slope are constant are identified as targets, shown in figure (c) (d) of 4 and 5, because the same mixing matrix set weights to each sample point. As noise or interference signals are not continuous, their slopes of phase variations cannot remain constant over the whole integration time.

## 5. CONCLUSIONS

In this paper, a Tree-structure based sparse-UBSS (TUBSS) method is proposed and applied to Passive Wi-Fi radar multi-target detection. From the simulation results, TUBSS is able to help identify two targets moving both in opposite and same directions using only one receiver, even if the velocity difference is only 0.5 m/s. In addition, robust ICA using two receivers provides slightly better performance than the TUBSS when the velocities are in the opposite direction, however, the TUBSS outperforms the ICA when the velocities are in the same direction. The proposed method is verified by both simulation and real experiments results using two targets moving in opposite directions. It has been shown that targets can be identified using a three-depth TUBSS method even in a high interference indoor environment. This is the first application of this method to passive wireless detection as far as we are aware and should significantly improve target identification in real world noisy indoor scenarios.

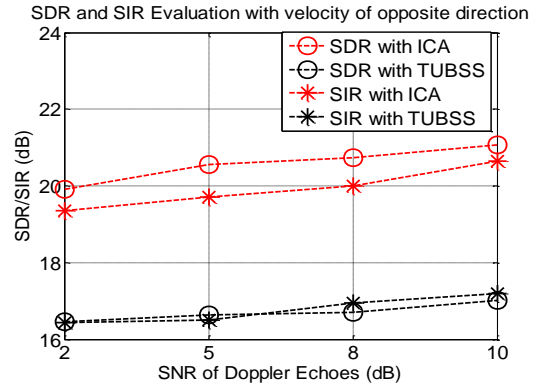


Figure 1 Evaluation of separation of scenario 1

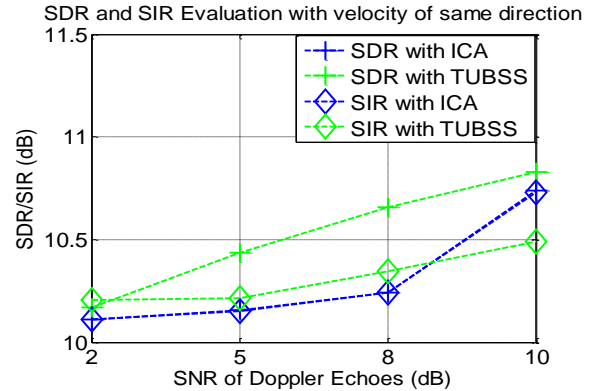


Figure 2 Evaluation of separation of scenario 2

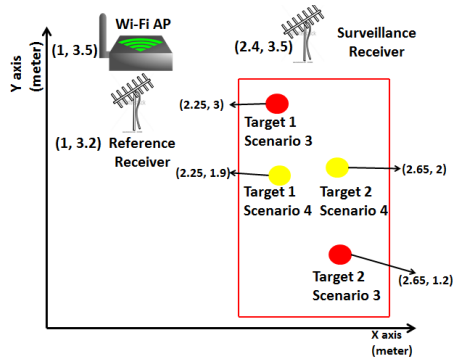


Figure 3 Experimental Scenarios 3 and 4

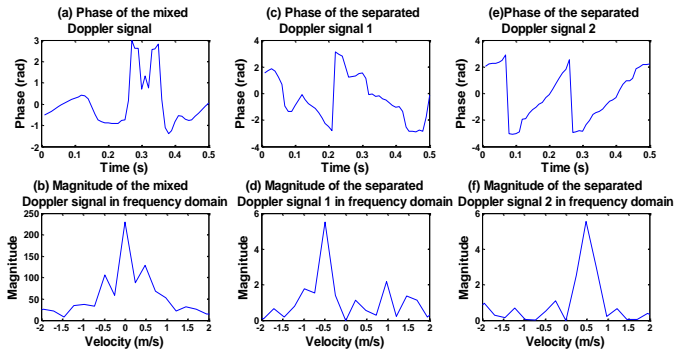


Figure 4 TUBSS result of experiment data of scenario 3 with similar signal source powers

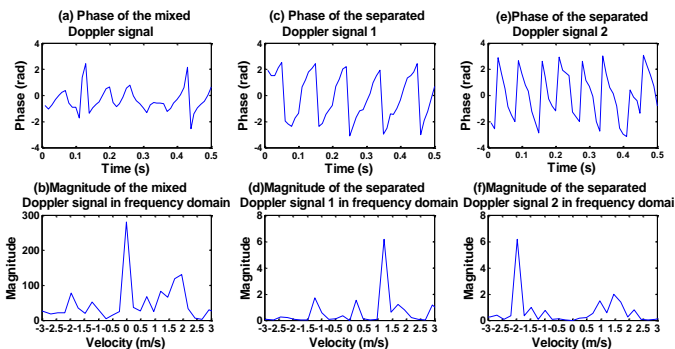


Figure 5 Sparse-UBSS result of experiment data of scenario 4 with different signal source powers

## REFERENCES

[1] D. K. P. Tan, H. Sun, Y. Lu, M. Lesturgie, and H. L. Chan, "Passive radar using Global System for Mobile communication signal: theory, implementation and measurements," *Radar, Sonar and Navigation, IEE Proceedings -*, vol. 152, pp. 116-123, 2005.

[2] K. Chetty, G. E. Smith, and K. Woodbridge, "Through-the-Wall Sensing of Personnel Using Passive Bistatic WiFi Radar at Standoff Distances," *Geoscience and Remote Sensing, IEEE Transactions on*, vol. 50, pp. 1218-1226, 2012.

[3] C. Qingchao, T. Bo, K. Woodbridge, and K. Chetty, "Indoor target tracking using high doppler resolution passive Wi-Fi radar," in *Acoustics, Speech and Signal Processing (ICASSP), 2015 IEEE International Conference on*, 2015, pp. 5565-5569.

[4] B. Tan, K. Woodbridge and K. Chetty, "A wireless passive radar system for real-time through-wall movement detection," in *IEEE Transactions on Aerospace and Electronic Systems*, vol. 52, no. 5, pp. 2596-2603, October 2016.

[5] H. A. Harms, L. M. Davis, and J. Palmer, "Understanding the signal structure in DVB-T signals for passive radar detection," in *Radar Conference, 2010 IEEE*, 2010, pp. 532-537.

[6] P. E. Howland, "Target tracking using television-based bistatic radar," *Radar, Sonar and Navigation, IEE Proceedings -*, vol. 146, pp. 166-174, 1999.

[7] Q. Chen, B. Tan, K. Chetty, and K. Woodbridge, "Activity Recognition Based on Micro-Doppler Signature with In-Home Wi-Fi," *arXiv preprint arXiv:1611.01801*, 2016.

[8] T. Bo, A. Burrows, R. Piechocki, I. Craddock, C. Qingchao, K. Woodbridge, et al., "Wi-Fi based passive human motion sensing for in-home healthcare applications," in *Internet of Things (WF-IoT), 2015 IEEE 2nd World Forum on*, 2015, pp. 609-614.

[9] F. Adib, Z. Kabelac, D. Katabi, and R. C. Miller, "3d tracking via body radio reflections," in *11th USENIX Symposium on Networked Systems Design and Implementation (NSDI 14)*, 2014, pp. 317-329.

[10] F. Adib, Z. Kabelac, and D. Katabi, "Multi-person motion tracking via RF body reflections," 2014.

[11] P. E. Howland, D. Maksimiuk, and G. Reitsma, "FM radio based bistatic radar," *Radar, Sonar and Navigation, IEE Proceedings -*, vol. 152, pp. 107-115, 2005.

[12] S. Makeig, A. J. Bell, T.-P. Jung, and T. J. Sejnowski, "Independent component analysis of electroencephalographic data," in *Advances in neural information processing systems*, 1996, pp. 145-151.

[13] T.-W. Lee, M. S. Lewicki, and T. J. Sejnowski, "ICA mixture models for unsupervised classification of non-Gaussian classes and automatic context switching in blind signal separation," *IEEE Transactions on Pattern Analysis and Machine Intelligence*, vol. 22, pp. 1078-1089, 2000.

[14] F. Feng and M. Kowalski, "Hybrid model and structured sparsity for under-determined convolutive audio source separation," in *Acoustics, Speech and Signal Processing (ICASSP), 2014 IEEE International Conference on*, 2014, pp. 6682-6686.

[15] J. Bobin, J.-L. Starck, Y. Moudon, and M. J. Fadili, "5 Blind Source Separation: The Sparsity Revolution," *Advances in Imaging and Electron Physics*, vol. 152, pp. 221-302, 2008.

[16] P. Bofill and M. Zibulevsky, "Underdetermined blind source separation using sparse representations," *Signal processing*, vol. 81, pp. 2353-2362, 2001.

[17] J. E. Palmer, H. A. Harms, S. J. Searle, and L. M. Davis, "DVB-T passive radar signal processing," *Signal Processing, IEEE Transactions on*, vol. 61, pp. 2116-2126, 2013.

[18] J. Sun, J. Lu, T. Xu, and J. Bi, "Multi-view sparse co-clustering via proximal alternating linearized minimization," in *Proceedings of the 32nd International Conference on Machine Learning (ICML-15)*, 2015, pp. 757-766.

[19] J. Bolte, S. Sabach, and M. Teboulle, "Proximal alternating linearized minimization for nonconvex and nonsmooth problems," *Mathematical Programming*, vol. 146, pp. 459-494, 2014.

[20] C. Cook, *Radar signals: An introduction to theory and application*: Elsevier, 2012.

[21] S. H. Baloch, H. Krim, and M. G. Genton, "Robust independent component analysis," in *Statistical Signal Processing, 2005 IEEE/SP 13th Workshop on*, 2005, pp. 61-64.

[22] C. Févotte, R. Gribonval, and E. Vincent, "BSS\_EVAL toolbox user guide--Revision 2.0," 2005.

[23] Colone, F., Pastina, D., Falcone, P., & Lombardo, P. (2014). WiFi-based passive ISAR for high-resolution cross-range profiling of moving targets. *IEEE Transactions on Geoscience and Remote Sensing*, 52(6), 3486-3501.

---